

Hydrogen-Bonding Characteristics and Unique Ring-Opening Polymerization Behavior of *Ortho*-Methylol Functional Benzoxazine

Kan Zhang,^{1,2} Pablo Froimowicz,^{2,3} Lu Han,² Hatsuo Ishida²

¹School of Materials Science and Engineering, Jiangsu University, Zhenjiang 212013, China

²Department of Macromolecular Science and Engineering, Case Western Reserve University, Cleveland, Ohio 44106

³Design and Chemistry of Macromolecules Group, Institute of Technology in Polymers and Nanotechnology (ITPN), School of Engineering, University of Buenos Aires, Buenos Aires, CP 1127AAR, Argentina

Correspondence to: H. Ishida (E-mail: hxi3@cwru.edu) or P. Froimowicz (E-mail: pxf106@case.edu)

Received 7 July 2016; accepted 29 July 2016; published online 00 Month 2016

DOI: 10.1002/pola.28253

ABSTRACT: Monofunctional benzoxazine with *ortho*-methylol functionality has been synthesized and highly purified. The chemical structure of the synthesized monomer has been confirmed by ¹H and ¹³C nuclear magnetic resonance spectroscopy (NMR), Fourier transform infrared spectroscopy (FT-IR) and elemental analysis. One-dimensional (1D) ¹H NMR is used with respect to varied concentration of benzoxazines to study the specific nature of hydrogen bonding in both *ortho*-methylol functional benzoxazine and its *para* counterpart. The

polymerization behavior of benzoxazine monomer has been also studied by *in situ* FT-IR and differential scanning calorimetry, experimentally supporting the polymerization mechanism of *ortho*-methylol functional benzoxazine we proposed before. © 2016 Wiley Periodicals, Inc. *J. Polym. Sci., Part A: Polym. Chem.* **2016**, *00*, 000–000

KEYWORDS: benzoxazine; hydrogen-bonding; ring-opening polymerization; thermosets; functionalization of polymers

INTRODUCTION Benzoxazine resin is an important thermosetting resin widely used in industrial applications, such as in electronic packaging materials, materials for aerospace, adhesives, and other transportation applications, as well as ballistics.^{1,2} It has been extensively reviewed due to its outstanding advantages.^{3–6} The most interesting and unique characteristic of this class of polymers is their extraordinarily rich molecular design flexibility that allows designing a variety of molecular structures to tailor the desired properties. Additionally, benzoxazine monomers can be easily synthesized from various phenols, amines, and formaldehyde. This versatile synthetic method has allowed development of various benzoxazines having functional groups such as amide,^{7–9} imide,^{9–11} allyl,^{12,13} nitrile,¹⁴ furyl,¹⁵ and benzoxazole,¹⁶ which were effectively used for various chemical modifications of the benzoxazine monomers and the corresponding polybenzoxazines including cross-linking reactions.

Polybenzoxazines can typically be produced via cationic ring-opening polymerization by heating benzoxazine monomers without added initiator and/or catalyst in the temperature range of 150–220 °C. However, some applications require lower polymerization temperature than this typical range. Several benzoxazines and naphthoxazines containing hydroxyl group have been developed.^{17,18} These literatures

described convenient use of hydroxyl group for polycondensation and initiation of ring-opening of lactone. Thermally induced polymerizations of benzoxazines containing a 2-(2-hydroxyethoxy)ethyl group have also been studied.¹⁹ The polymerizations of these monomers proceeded smoothly at relatively low temperature may be due to the presence of hydrogen bonding offered by OH group. In addition, Endo and coworkers reported polymerization behavior of 3-(2-hydroxyethyl)-1,3-benzoxazine. They proposed that the nucleophilic hydroxyl group would highly activate the ring-opening of benzoxazine moiety in an intramolecular manner.²⁰ Recently, Baqar et al. synthesized a series of methylol functional benzoxazine monomers with different hydroxybenzyl alcohol isomers. They proposed that the highest catalytic effect observed was in fact caused by the presence of an intramolecular hydrogen bond between the hydroxyl group placed on *ortho* position and the oxygen in the oxazine ring, which led to acceleration of the polymerization.²¹ As can be seen from the previous examples, there are various effects which have been hypothesized to be the driving force and/or the cause for the lower polymerization temperature of benzoxazines having hydroxyl group.

The intramolecular hydrogen bonding hypothesis can explain the experiment results and let propose polymerization mechanisms. However, the intramolecular hydrogen-bonding

system in benzoxazines has rarely been studied and the intramolecular hydrogen-bonding in hydroxyl functional benzoxazines still has not been experimentally demonstrated to exist.²² Moreover, it is known that impurities that exist during the synthesis of benzoxazine monomer acts as an efficient initiator and/or catalyst. Therefore, it is essential that a highly purified monomer must be used to study mechanistic aspects of the ring-opening polymerization of benzoxazine. For this reason, we used only single-crystal samples of benzoxazine monomers that exhibit sharp differential scanning calorimetry (DSC) melting endothermic peaks in this study.

The main purpose of this work is to experimentally study the intramolecular hydrogen-bonding interactions that are possible for the hydroxyl-containing benzoxazine compound **oHBA-a** (Fig. 1). In this compound, the methylol group is placed at the 8-position (*ortho* with respect to the oxygen in the oxazine ring) in the benzoxazine nucleus. For comparison, **pHBA-a** (Fig. 1), the methylol groups is placed at the 6-position (*para* with respect to the oxygen in the oxazine ring) was also investigated. The results of this study will provide for the first time experimental data demonstrating the existence of such intramolecular hydrogen bonding only in *ortho*-methylol functional benzoxazine. At the same time, our discovery of the unique polymerization behavior of **oHBA-a** is described to further support the polymerization mechanism of *ortho*-methylol functional benzoxazine we proposed before, supplementing our earlier report on the synthesis and polymerization mechanism of methylol-functional benzoxazine monomers.²¹

EXPERIMENTAL

Materials

2-Hydroxybenzyl alcohol (**oHBA**) (99%), 4-Hydroxybenzyl alcohol (**pHBA**) (98%), aniline, and paraformaldehyde (96%) were used as received from Sigma-Aldrich. Ethyl acetate, toluene, hexane, chloroform, 1,4-dioxane, sodium hydroxide (NaOH), and sodium sulfate were obtained from Fisher scientific and used as received. 3-phenyl-3,4-dihydro-2H-benzo[e][1,3]oxazine (**PH-a**) and (3-phenyl-3,4-2H-benzo[e][1,3]oxazin-6-yl)-methanol (**pHBA-a**) were prepared following the methods developed in our laboratory, which were published elsewhere.²¹

Characterization

¹H and ¹³C nuclear magnetic resonance (NMR) spectra were acquired on a Varian Oxford AS600 at a proton frequency of 600 MHz and its corresponding carbon frequency of 150.864 MHz. The average number of transients for ¹H and ¹³C NMR measurement was 64 and 1024, respectively. A relaxation time of 10 s was used for the integrated intensity determination of ¹H NMR spectra. Fourier transform infrared (FT-IR) spectra were obtained using a Bomem Michelson MB100 FT-IR spectrometer, which was equipped with a deuterated triglycine sulfate (DTGS) detector and a dry air purge unit. Coaddition of 64 scans was recorded at a resolution of 4 cm⁻¹. A TA Instruments Differential Scanning Calorimeter

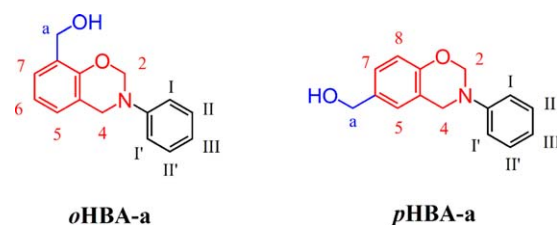


FIGURE 1 Chemical Structures and full numbering of **oHBA-a** and **pHBA-a** for complete identification of each position in the benzoxazine nuclei and of every position of each substituent present in the molecule. [Color figure can be viewed in the online issue, which is available at wileyonlinelibrary.com.]

Model 2920 was used with a heating rate of 10 °C/min and a nitrogen flow rate of 60 mL/min. In the analyses to determine the activation energy of benzoxazine polymerization, the samples (2.0 ± 0.5 mg) were scanned at different heating rates, specifically 2, 5, 10, 15, and 20 °C/min. All samples were sealed in hermetic aluminum pans with lids.

Synthesis of (3-Phenyl-3,4-dihydro-2H-benzo[e][1,3]oxazin-8-yl)Methanol (**oHBA-a**)

Into a 50 mL round flask were added 1,4-dioxane (20 mL), aniline (1.4 g, 15 mmol), **oHBA** (1.86 g, 1.5 mmol), and paraformaldehyde (0.96 g, 30 mmol). The mixture was stirred at 100 °C for 48 h, and subsequently cooled to room temperature. Then the product was concentrated using a rotary evaporator. The product was then re-dissolved in chloroform and washed by water for three times. The chloroform solution was dried over anhydrous sodium sulfate to obtain the crude product. Crude product was fractionated by the column chromatography (eluent: hexanes and ethyl acetate, volume ratio = 4:1). After solvent removal, the resulting white crystals were purified by recrystallizing in chloroform (yield 58%). ¹H NMR (DMSO-*d*₆), ppm: δ = 4.40 (d, -CH₂-OH), 4.62 (s, Ar-CH₂-N, oxazine), 4.93 (t, -OH), 5.41 (s, O-CH₂-N, oxazine), 6.90–7.24 (m, Ar). IR spectra (KBr), cm⁻¹: 3306 and 3212 (stretching of OH of methylol), 1498 (stretching of tri-substituted benzene ring), 1221 (Ar-O-C asymmetric stretching), 929 (out-of-plane C-H of benzene ring to which oxazine ring is attached).

Anal. calcd. for C₁₅H₁₅NO₂: C, 74.69%; H, 6.22%; N, 5.84%. Found: 74.29%; H, 6.30%; N, 5.71%.

RESULTS AND DISCUSSION

Synthesis of *Ortho*-Methylol Functional Benzoxazine Monomer

Prior to this study, a series of methylol functional benzoxazine monomers with different hydroxylbenzyl alcohol isomers have been reported aiming to understand the isomeric effect on ring-opening polymerization of benzoxazine.²¹ However, the purity of **oHBA-a** monomers used in the previous work was not sufficient due to the existence of the intramolecular hydrogen bonding in **oHBA**, leading the difficulties of ring-closing of oxazine ring. The potential impurities, such as phenols, amines, and benzoxazine oligomers all show the

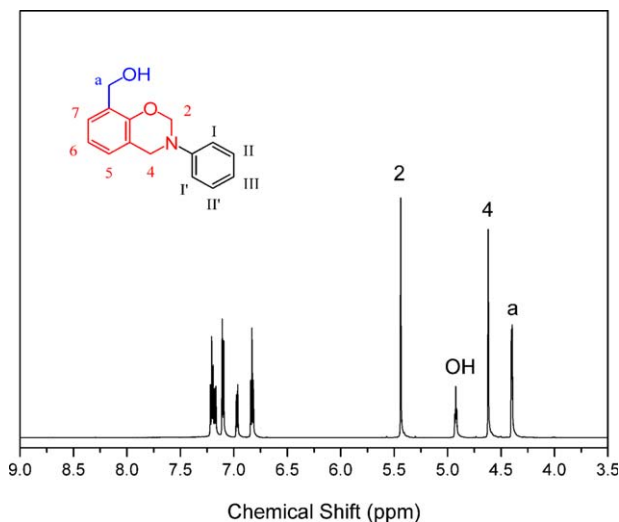


FIGURE 2 ^1H NMR spectra of *ortho*-methylol functional benzoxazine (**oHBA-a**) in $\text{DMSO-}d_6$. [Color figure can be viewed in the online issue, which is available at wileyonlinelibrary.com.]

promoting effect on the ring-opening polymerization of benzoxazines.^{23,24} Therefore, column chromatograph followed by exhaustive recrystallization were used to separate the impurities in order to obtain high purity benzoxazine monomers in this study.

Formation of the structures of **oHBA-a** was confirmed using ^1H NMR, ^{13}C NMR, FT-IR, and elemental analysis. Figure 2 shows the ^1H NMR spectrum of **oHBA-a**. Typically, benzoxazine monomers have two singlet resonances with equal integration values in ^1H NMR spectra due to the two $-\text{CH}_2-$ in the oxazine ring. The characteristic resonances attributed to the benzoxazine structure, $\text{Ar-CH}_2\text{-N-}$ and $-\text{O-CH}_2\text{-N-}$ are observed at 4.62 and 5.41 ppm, respectively. Also, the ^1H NMR spectra confirm the presence of methylol group ($-\text{CH}_2\text{OH}$) from the resonances of $-\text{CH}_2\text{-O}$ and hydroxyl of methylol group at 4.40 and 4.93 ppm, respectively.

^{13}C NMR analysis was also performed to further confirm the structures of **oHBA-a** as shown in Figure 3. The characteristic carbon resonances of oxazine ring appear at 49.49 and 79.40 ppm for $\text{Ar-CH}_2\text{-N-}$ and $-\text{O-CH}_2\text{-N-}$, respectively. The resonance at 58.06 ppm is assigned to the $-\text{CH}_2\text{OH}$ of methylol group.

The FT-IR spectrum of **oHBA-a** using the KBr pellet method is shown in Figure 4. The hydroxyl stretching vibration region in the FT-IR spectrum of **oHBA-a** shows bands at 3306 and 3212 cm^{-1} , corresponding to the stretch vibrations of the free $-\text{OH}$ groups and hydrogen-bonded $-\text{OH}$ groups, respectively. In addition, band characteristic of anti-symmetric trisubstituted benzene that appear in **oHBA-a** at 1498 cm^{-1} confirm the incorporation of methylol group into benzoxazine monomer. Also, the presence of the benzoxazine ring aromatic ether in the monomers is indicated by bands centered at 1221 cm^{-1} , which is due to the C-O-C asymmetric stretching modes.²⁵ Furthermore, the characteristic out-

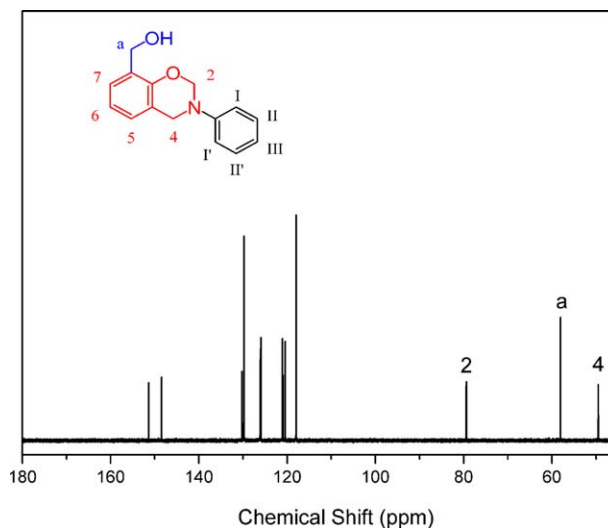


FIGURE 3 ^{13}C NMR spectrum of **oHBA-a** in $\text{DMSO-}d_6$. [Color figure can be viewed in the online issue, which is available at wileyonlinelibrary.com.]

of-plane absorption mode of benzene with an attached oxazine ring is located at 929 cm^{-1} .²⁶ The excellent agreement between the calculated and observed data from the elemental analysis of the purified sample, it shows that the targeted compound **oHBA-a** was obtained in high purity.

^1H NMR Studies in Solution

In order to better understand the hydrogen-bonding interactions in **oHBA-a**, and for comparison, **pHBA-a** was also studied.

In ^1H NMR, the quality of alcohol signals usually depends on the solvent used. In general, and for the very same OH group, non-protic solvents provide better resolution than solvents presenting the ability to carry out intermolecular proton-deuterium exchange with the substrate. Clearly, more acidic solvents produce higher intermolecular proton-deuterium exchange rates. For example, when D_2O and

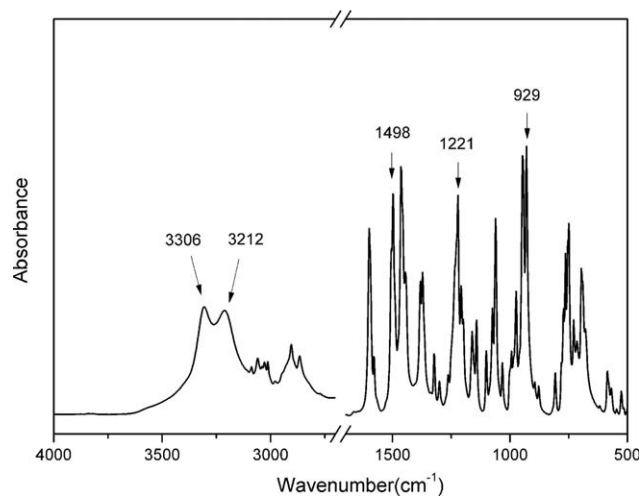


FIGURE 4 FT-IR spectrum of **oHBA-a**.

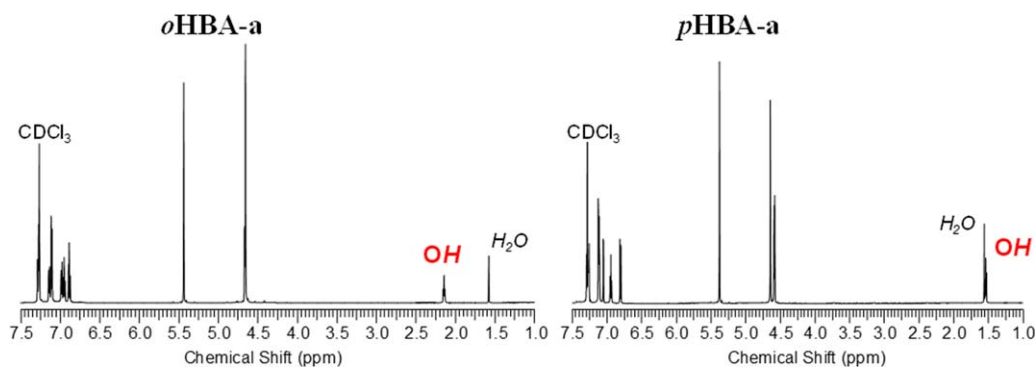


FIGURE 5 Representative ^1H NMR spectra of both compounds **oHBA-a** and **pHBA-a**. Spectra were recorded using CDCl_3 as solvent and at 25°C . [Color figure can be viewed in the online issue, which is available at wileyonlinelibrary.com.]

deuterated alcohols are used as solvents for alcohol-containing compounds the OH groups are usually not detected in the ^1H NMR spectrum. This “disappearance” of the OH signal in some solvents is often smartly exploited to detect not only the presence of alcohols, but in occasions also to distinguish between primary, secondary and tertiary alcohols. However, if a solvent that is less acidic than D_2O but that still performs this intermolecular proton-deuterium exchange, such as CDCl_3 , is used instead, broad signals normally not integrable for the OH groups are seen in the spectrum. This broadening is caused by the rate of the proton-deuterium exchange, which is much lower in CDCl_3 than in D_2O or deuterated alcohols, due to its lower acidity. This is, however, applicable to free alcohol groups exhibiting high mobility given by their good solvation in the solvent. Nevertheless, the opposite situation happens when the OH groups are somehow involved in different interactions or stable molecular motifs. This causes a diminution of their mobility and/or accessibility, thus impeding their rate of intermolecular proton-deuterium exchange, which in turn favors a better resolution of the OH signals. Sometimes, it is even possible to measure the coupling constant for the OH signal with the corresponding neighboring protons; however, this is certainly not necessarily the case for all systems. For a single system, for instance, it can be seen on the one hand that protons inside of aggregates, nanoparticles or micelles,²⁷ are mostly not detected in the spectrum since their mobility are highly decreased causing the broadening of their signals on the order of hundreds of Hz thus making them imperceptible.²⁸ The reactivity of OH and NH groups is also affected depending on their placement in these systems, low exposure to the solvent gives rise to less accessibility, and thus their reactivity is highly reduced.^{29–31} And, on the other hand, protons that are on the surface and exposed to the solvent are easily observed since they are well solvated.³²

As shown in Figure 5, however, well defined and resolved signals of the OH groups using CDCl_3 as the solvent for the simple ^1H NMR spectra of the herein studied compounds **oHBA-a** and **pHBA-a** were observed. This indicates that the OH groups are involved in some interactions or forming stable structural motifs, and yet solvated. This is consistent

with the presence of hydrogen-bonding systems in each sample. Nevertheless, no further information about the nature of these hydrogen-bonding can be concluded without further and complementary analysis. In this regard, it has been reported that hydrogen-bonding has also the effect of shifting the OH signals downfield (high frequency, higher chemical shift).³³ The magnitude of this shifting has also been exploited as a manner to distinguish between inter- and intramolecular hydrogen-bonding systems.³⁴ Moreover, inter- and intramolecular hydrogen-bonds can be further studied and better identified using simple ^1H NMR experiments, by evaluating the corresponding chemical shifts for each OH signal as a function of the concentration.^{35,36}

Figure 6 shows a summary of the chemical shifts for the OH signals belonging to **oHBA-a** and **pHBA-a** as a function of their concentrations, obtained from the ^1H NMR spectra using CDCl_3 as a solvent. It can be seen that the OH signal belonging to **pHBA-a** experienced an important chemical

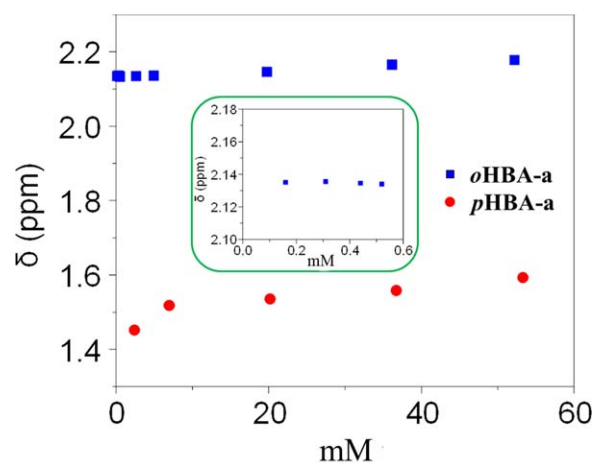


FIGURE 6 Chemical shift summary of the OH signal belonging to **oHBA-a** (■) and **pHBA-a** (●) as a function of the concentration. Spectra recorded using CDCl_3 as solvent at 25°C . Inset: magnification of the plot at concentration between 0.00 and 0.60 mM, where only **oHBA-a** signals were detected. [Color figure can be viewed in the online issue, which is available at wileyonlinelibrary.com.]

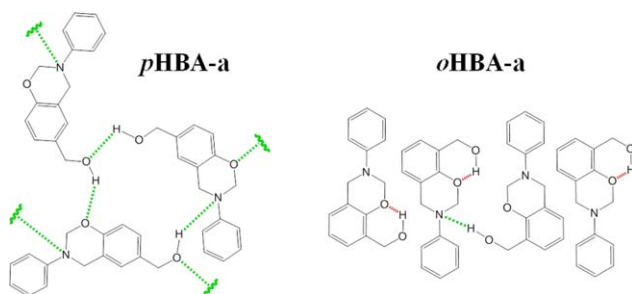


FIGURE 7 Proposed hydrogen-bonding interactions in **pHBA-a** and **oHBA-a**. Long green dotted lines depict possible intermolecular hydrogen-bonding in both **pHBA-a** and **oHBA-a**, while red dotted lines represent the intramolecular hydrogen-bonding only present in **oHBA-a**. [Color figure can be viewed in the online issue, which is available at wileyonlinelibrary.com.]

shift toward greater δ (downfield) upon increasing the concentration, while the *OH* signal of **oHBA-a** shifted only slightly for the same range of concentrations. A closer look at concentrations below 0.60 mM (inset in Fig. 6) shows no changes in the chemical shifts of the *OH* belonging to **oHBA-a**, which remains constant even at very high dilutions. In the case of **pHBA-a**, however, the *OH* signal is no longer seen at these high dilutions.

These results strongly suggest the existence of hydrogen-bonding in both molecules (**oHBA-a** and **pHBA-a**), although different in nature (Fig. 7).

The clear dependence of the *OH* chemical shift for **pHBA-a** upon concentration is indication of intermolecular hydrogen-bonding. The higher the concentration, the higher the downfield chemical shift, due to the decreased in-average hydrogen-bonding distance between different molecules of **pHBA-a**, strengthening the interaction. At concentrations below 0.60 mM, however, the *OH* signal is no longer seen, probably because of the high rate of proton-deuterium exchange that could take place at that diluted conditions by the loss of intermolecular interactions among the benzoxazine molecules. At these low concentrations, only the intermolecular interaction between the benzoxazine and solvent molecules exist.

In the case of **oHBA-a**, however, there seems to be a more complex situation than for **pHBA-a** depending on the concentration range. First, and in contrast to what happens with the *OH* signal in **pHBA-a**, in highly diluted solution the *OH* signal is clearly seen and is independent of the concentration. This is a strong indication that the hydrogen-bond in **oHBA-a** is intramolecular. Nevertheless, intermolecular hydrogen-bond interactions start to be noticeable at concentration higher than 2.50 mM since upon this concentration slight concentration dependence is perceptible. This weak dependence of the chemical shifts of the *OH* belonging to **oHBA-a** compared to those from **pHBA-a** is explained by the lower availability of the *OH* groups from **oHBA-a** to

participate in intermolecular hydrogen-bonding since they are already forming intramolecular ones. This observation of complex behavior is, at a first glance, counterintuitive as ordinary strong intramolecular hydrogen bonds shows independence of *OH* chemical shift as a function of concentration. It is possible that the six-membered intramolecular hydrogen-bond observed in this molecule is not that strong. Thus, the nitrogen atom in the oxazine ring can disturb the preexisting hydrogen-bonding and break up a small fraction of the intramolecular hydrogen-bonds forming intermolecular hydrogen-bonds when the intermolecular distance becomes shorter at high concentrations.

Figure 8 shows a typical ^1H NMR spectrum of **oHBA-a** that is highly diluted using CDCl_3 as solvent. Given the very low concentration, two regions of interest are expanded for clarity and presented next. The first region from 4.5 to 5.5 ppm shows the two $-\text{CH}_2-$ belonging to the oxazine ring of the benzoxazine, as well as the $-\text{CH}_2-\text{OH}$ in *ortho* position respect to the oxygen of the oxazine ring. This last signal is overlapped with the one from $\text{Ph}-\text{CH}_2-\text{N}=\text{}$ present at 4.65 ppm. The second region from 2.0 to 2.3 ppm allows us to see a very nicely resolved triplet belonging to the *OH* signal.

A second piece of supporting evidence for the intramolecular hydrogen-bonding in **oHBA-a** is obtained from the ^1H NMR spectra at very low concentrations where the dependence upon concentration is no longer observed. As mentioned earlier, using CDCl_3 as solvent and at very low concentration the *OH* signals are typically seen as broad signals usually not integrable. Occasionally, *OH* signals might not be seen due to a high rate of intermolecular proton-deuterium exchange between the substrate and the solvent. However, in the case of compound **oHBA-a** at low concentrations, discrete triplets for the *OH* signals are observed, indicating that those *OH*

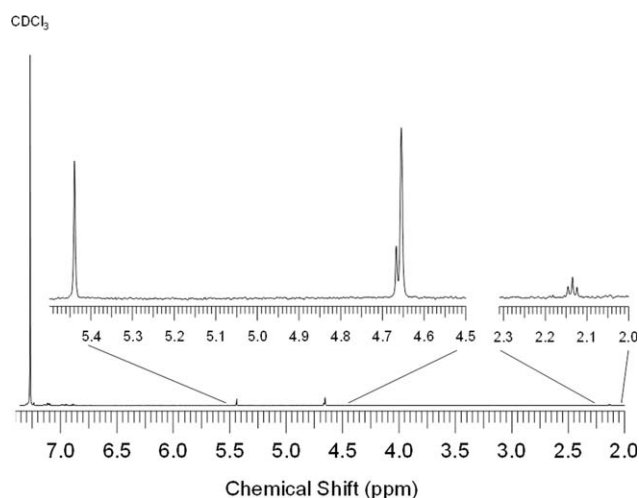


FIGURE 8 ^1H NMR spectrum of **oHBA-a**, using CDCl_3 as solvent at a concentration of 0.16 mM. The expanded region between 4.5 and 5.5 ppm shows the two $-\text{CH}_2-$ belonging to the oxazine ring and the $-\text{CH}_2-\text{OH}$, which is overlapped with the signal $\text{Ph}-\text{CH}_2-\text{N}=\text{}$, while the expanded region between 2.0 and 2.3 ppm shows the *OH* signal.

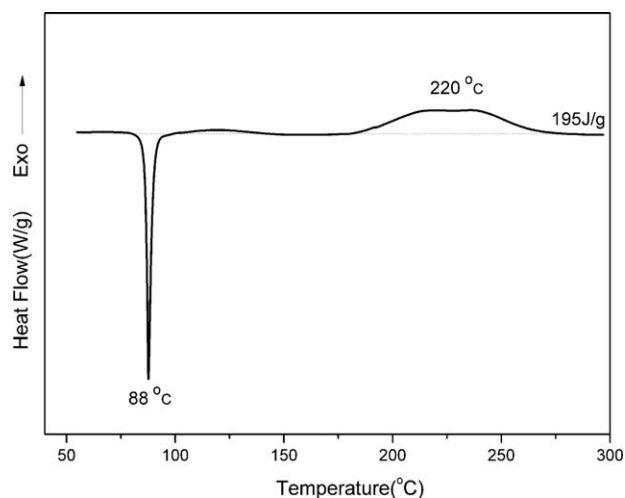


FIGURE 9 DSC polymerization behavior of monofunctional benzoxazine monomers.

groups are not free but involved in hydrogen-bonded systems. The facts that these discrete and well resolved triplets for the *OH* groups are seen even at high dilution (Fig. 8) as well as their chemical shifts do not move upon increasing the concentration (Fig. 6) are strong evidence supporting the existence of intramolecular hydrogen-bonding in **oHBA-a**.

A third piece of supporting evidence for the intramolecular hydrogen-bonding in **oHBA-a** is obtained after performing straightforward recognition of exchangeable protons studies by ^1H NMR at very low concentrations as control experiments. The protocol is as follows: a simple ^1H NMR spectrum is recorded and fully assigned using CDCl_3 as solvent. Then, two drops of D_2O are added to the same sample, which is then shaken and allowed to separate into two phases (the organic phase remains at the bottom as CDCl_3 is denser than water). Finally, the second spectrum is recorded and fully assigned. The possible consequences of this control experiment are (a) labile acidic protons belonging to the substrate will be exchanged and no longer seen on the second spectrum; (b) no signals are vanished on the second spectrum, demonstrating that no labile acidic protons are present; or (c) known labile acidic protons present in the substrate are strongly participating in hydrogen-bonding, and therefore are unchangeable due to their involvement in that interaction. The last situation was observed when a highly diluted sample of **oHBA-a** was studied. This result is supporting once again the intramolecular hydrogen-bonding system present only in **oHBA-a**.

Polymerization Behavior of **oHBA-a**

The polymerization behavior of *ortho*-methylol functional benzoxazine monomer was studied by DSC as depicted in Figure 9 and the results are summarized in Table 1. In addition, the DSC thermograms for the unsubstituted **PH-a** as well as the *para*-methylol functional benzoxazine **pHBA-a**, which have been reported elsewhere,²¹ are also summarized in Table 1 for comparison.

TABLE 1 Results From the DSC Analysis and Literature of Benzoxazine Monomers

Monomer	Onset Temp (°C)	Max Temp (°C)	Heat of Polymerization (J/g)	Ref.
oHBA-a	185	220	195	This work
pHBA-a	205	231	241	21
PH-a	237	255	336	21

The thermogram in Figure 9 shows a very sharp endothermic peak at 88 °C, indicating the excellent purity of **oHBA-a**. Moreover, **oHBA-a** shows the onset of the ring-opening polymerization at 185 °C with its maximum centered at 220 °C. Comparing to the unsubstituted **PH-a**, benzoxazines with the methylol substituent have significantly reduced the onset and maxima of polymerization temperature. The remarkably high reactivity of methylol functional benzoxazine could be caused by participation of polar and potentially nucleophilic hydroxyl group from the view of electronic effects by the substituents on the polymerization mechanism. Additionally, **oHBA-a** is much more reactive than **pHBA-a** to imply that the *ortho* position of the hydroxyl group accelerating the polymerization more effectively compared with the *para* position. Combining with the ^1H NMR analysis of hydrogen bonds in solution, the presence of intramolecular hydrogen bonding between an methylol linkage and the adjacent oxazine ring of **oHBA-a** would act as an incentive to further stimulate the ring-opening polymerization. Also, the DSC results in this study further support our previous proposed mechanism where, the intramolecular hydrogen bonding ring activates the oxazine ring to open at lower temperature.²¹

Interestingly, the exothermic peak of **oHBA-a** is significant broader and the value for the polymerization heat is much lower compared with other traditional benzoxazine resins. The occurrence of methylol condensation reaction together

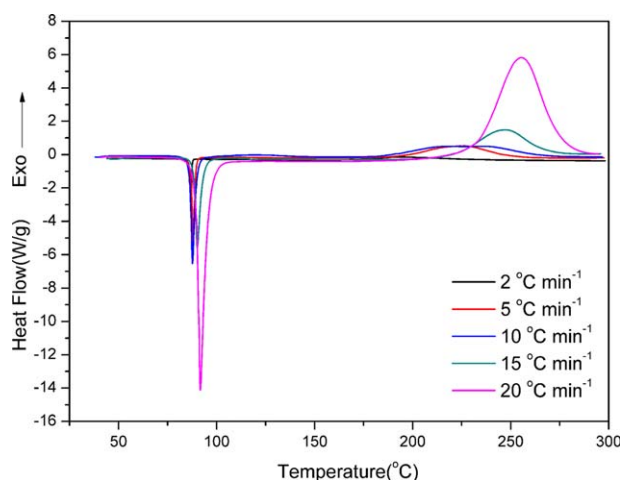


FIGURE 10 DSC curves of **oHBA-a** at different heating rates. [Color figure can be viewed in the online issue, which is available at wileyonlinelibrary.com.]

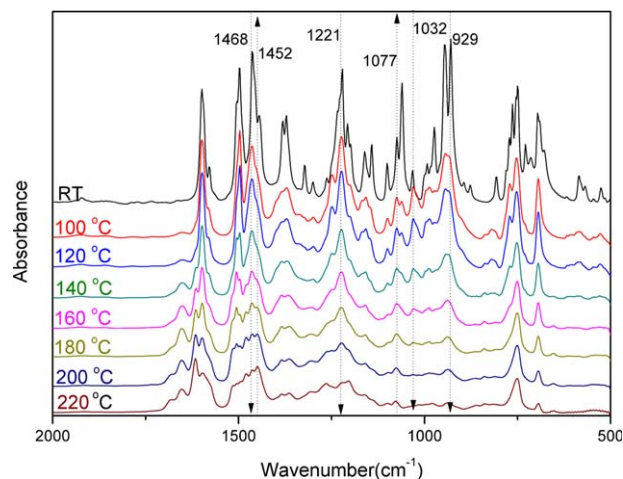


FIGURE 11 FT-IR spectra of oHBA-a after various thermal treatment. [Color figure can be viewed in the online issue, which is available at wileyonlinelibrary.com.]

with ring-opening polymerization of *ortho*-methylol bifunctional benzoxazine has been confirmed elsewhere.³⁷

Figure 10 shows the DSC thermograms of oHBA-a at different heating rates. Figure 10 also shows the initial polymerization temperature (T_i) and peak temperature (T_p) at different heating rates. Normally, the endothermic and exothermic peaks would shift to a higher temperature with the increase in heating rate for benzoxazine resins. However, the exothermic peak of oHBA-a does not follow the regulation as the normal traditional benzoxazine resins, showing clearly that another thermal event is involved in the ring-opening reaction.

For further insight, thermally accelerated polymerization of oHBA-a was also studied in detail by using FT-IR as depicted in Figure 11. The characteristic absorption bands at 1221 cm^{-1} (C-O-C asymmetric stretching modes) and 929 cm^{-1} (the out-of-plane bending vibration of C-H) gradually disappear from room temperature to $220\text{ }^\circ\text{C}$, supporting the ring-opening polymerization of oxazine ring. The typical absorption peak of methylol is observed at 1032 cm^{-1} due to the C-O stretching, whereas the condensation reaction can be followed through monitoring the CH_2 bending of the methylene bridge at 1468 cm^{-1} .³⁸ As shown in Figure 11, additional characteristic signals of methylene bridge C-H band at 1452 cm^{-1} are observed. During the polymerization, a decrease in characteristic absorption band centered at 1032 cm^{-1} due to the stretching of C-O (methylol) confirms the methylol condensation reaction. In addition, the methylene ether-type linkage at 1077 cm^{-1} appeared. Furthermore, an increased intensity of the band at 1452 cm^{-1} due to the CH_2 bending mode of methylene (CH_2) of methylol group confirms the occurrence of condensation reaction and the formation of methylene bridge.^{39,40} The FT-IR results further support the occurrence of both condensation reaction and ring-opening polymerization during thermal treatment of *ortho*-methylol functional benzoxazine.

Therefore, the above experimental results further and strongly support the *ortho*-methylol mechanisms for the crosslinking reaction which we have been reported elsewhere.²¹

CONCLUSIONS

The *ortho*-methylol functional benzoxazine monomer was successfully synthesized and highly purified. The concentration dependent 1D ^1H NMR results indicate the existence of the intramolecular hydrogen bonding in *ortho*-methylol functional benzoxazine. The DSC and FT-IR results show that the occurrence of both condensation reaction and ring-opening polymerization during thermal treatment of *ortho*-methylol functional benzoxazine. Both experimental studies, hydrogen-bonding interactions and polymerization, further and strongly support the *ortho*-methylol mechanisms for the crosslinking reaction we proposed.

REFERENCES AND NOTES

- 1 F. Holly, A. C. Cope, *J. Am. Chem. Soc.* **1944**, *66*, 1875–1879.
- 2 X. Ning, H. Ishida, *J. Polym. Sci., Part A: Polym. Chem.* **1994**, *32*, 1121–1129.
- 3 H. Ishida, In *Handbook of Benzoxazine Resins*; H. Ishida, T. Aaga, Eds.; Elsevier: Amsterdam, **2011**, pp 3-81.
- 4 C. P. R. Nai, *Prog. Polym. Sci.* **2004**, *29*, 401–498.
- 5 N. N. Ghosh, B. Kiskan, Y. Yagci, *Prog. Polym. Sci.* **2007**, *32*, 1344–1391.
- 6 T. Takeichi, T. Kawauchi, T. Agag, *Polym. J.* **2008**, *40*, 1121–1231.
- 7 T. Agag, C. R. Arza, F. H. J. Manrer, H. Ishida, *J. Polym. Sci., Part a: Polym. Chem.* **2011**, *49*, 4335–4342.
- 8 T. Agag, J. Liu, R. Graf, H. W. Spiess, H. Ishida, *Macromolecules* **2012**, *45*, 8991–8997.
- 9 K. Zhang, H. Ishida, *Polym. Chem.* **2015**, *5*, 2541–2550.
- 10 S. N. Kolanadiyil, J. Bigwe, I. K. Varma, *React. Funct. Polym.* **2013**, *73*, 1544–1552.
- 11 K. Zhang, J. Liu, S. Ohashi, X. Liu, Z. Han, H. Ishida, *J. Polym. Sci., Part a: Polym. Chem.* **2015**, *53*, 1330–1338.
- 12 M. Ergin, B. Kiskan, B. Gacal, Y. Yagci, *Macromolecules* **2007**, *40*, 4724–4727.
- 13 T. Agag, T. Takeichi, *Macromolecules* **2001**, *34*, 7257–7263.
- 14 H. Qi, H. Ren, G. Pan, Y. Zhuang, F. Huang, L. Du, *Polym. Adv. Technol.* **2009**, *20*, 268–272.
- 15 Y. L. Liu, C. I. Chou, *J. Polym. Sci., Part A: Polym. Chem.* **2005**, *43*, 5267–5282.
- 16 K. Zhang, Q. Zhuang, Y. Zhou, X. Liu, G. Yang, Z. Han, *J. Polym. Sci., Part A: Polym. Chem.* **2012**, *50*, 5115–5123.
- 17 Y. C. Su, W. C. Chen, K. L. Ou, F. C. Chang, *Polymer* **2005**, *46*, 3758–3766.
- 18 B. Kiskan, Y. Yagci, *Polymer* **2005**, *46*, 11690–11697.
- 19 B. Kiskan, B. Koz, Y. Yagci, *J. Polym. Sci., Part A: Polym. Chem.* **2009**, *47*, 6995–6961.
- 20 R. Kudoh, A. Sudo, T. Endo, *Macromolecules* **2010**, *43*, 1185–1187.
- 21 M. Baqar, T. Agag, R. Huang, J. Maia, S. Qutubuddin, H. Ishida, *Macromolecules* **2012**, *45*, 8119–8125.

- 22** P. Froimowicz, K. Zhang, H. Ishida, *Chem. Eur. J.* **2016**, *22*, 2691–2707.
- 23** T. Orihara, Jpn Kokai Tokkyo Koho Patent 200086863A1, **2000**.
- 24** J. Q. Sun, W. Wei, Y. Z. Xu, J. H. Qu, X. D. Liu, T. Endo, *RSC Adv.* **2015**, *5*, 19048–19057.
- 25** T. Agag, T. Takeichi, *Macromolecules* **2003**, *36*, 6010–6017.
- 26** J. Dunkers, H. Ishida, *Spectrochim. Acta.* **1995**, *51 A*, 1061–1074.
- 27** P. Froimowicz, J. I. Paez, L. Gerbino, S. N. Ali, M. N. Belgacem, A. Gandini, M. C. Strumia, *Macromol. Res.* **2012**, *20*, 800–809.
- 28** I. Gitsov, K. L. Wooley, J. M. J. Frechet, *Angew. Chem. Int. Edit. Engl.* **1992**, *31*, 1200–1202.
- 29** A. Halabi, P. Froimowicz, M. C. Strumia, *Polym. Bull.* **2003**, *51*, 119–126.
- 30** P. Froimowicz, A. Gandini, M. Strumia, *Tetrahedron. Lett.* **2005**, *46*, 2653–2657.
- 31** P. Froimowicz, J. Paez, A. Gandini, N. Belgacem, M. Strumia, *Macromol. Symp.* **2006**, *245*, 51–60.
- 32** R. Sauer, P. Froimowicz, K. Scholler, J. M. Cramer, S. Ritz, V. Mailander, K. Landfester, *Chem. Eur. J.* **2012**, *18*, 5201–5212.
- 33** P. H. Che, F. Lu, X. Nie, Y. Z. Huang, Y. L. Yang, F. Wang, J. Xu, *Chem. Commun.* **2015**, *51*, 1077–1080.
- 34** P. Charisiadis, V. G. Kontogianni, C. G. Tsiafoulis, A. G. Tzakos, M. Siskos, I. P. Gerotheranassis, *Molecules.* **2014**, *19*, 13643–13682.
- 35** Y. Hisamatsu, Y. Fukumi, N. Shirai, S. Ikeda, K. Odashima, *Tetrahedron. Lett.* **2008**, *49*, 2005–2009.
- 36** L. X. Wang, B. Q. Hu, J. F. Xiang, J. Cui, X. Hao, T. L. Liang, Y. L. Tang, *Tetrahedron* **2014**, *70*, 8588–8591.
- 37** M. Baqar, T. Agag, H. Ishida, S. Outubuddin, *J. Polym. Sci., Part A: Polym. Chem.* **2012**, *50*, 2275–2286.
- 38** N. Gabilondo, M. Larranaga, C. Pena, M. A. Coruera, J. M. Echeverria, I. Mondragon, *J. Appl. Polym. Sci.* **2006**, *102*, 2623–2631.
- 39** A. Gardziella, L. A. Pilato, A. Knop, *Pehnolic Resins: Chemistry, Applications, Standardization, Safety and Ecology*; Springer: Berlin, **2000**; Chapter 6, pp 122–468.
- 40** A. Kaushik, P. Singh, G. Verma, J. Rekha, *Thermoplast. Compos. Mater.* **2010**, *23*, 79–97.